https://doi.org/10.5194/amt-2020-368
Preprint. Discussion started: 29 September 2020


Atmospheric Measurement Techniques Discussions

# Reducing cloud contamination in AOD measurements

Verena Schenzinger[1] and Axel Kreuter[1, 2]

[1]Institute for Biomedical Physics, Medical University Innsbruck, Innsbruck, Austria
[2]Luftblick OG, Innsbruck, Austria

**Correspondence:** Verena Schenzinger (verena.schenzinger@i-med.ac.at)

**Abstract.** We propose a new cloud screening method for sun photometry that is designed to effectively filter thin clouds. Our method is based on a k-nearest neighbour algorithm instead of scanning timeseries of aerosol optical depth. Using ten years of data from a precision filter radiometer in Innsbruck, we compare our new method and the currently employed screening technique. We exemplify the performance of the two routines in different cloud conditions. While both algorithms agree on the classification of a datapoint as clear or cloudy in a majority of the cases, the new routine is found to be more effective in flagging thin clouds. We conclude that this simple method can serve as a valid alternative for cloud detection, and discuss the generalizability to other observation sites.

## 1 Introduction

Sun photometry is one of the longest employed and robust measurement techniques for total column aerosol optical depth (AOD) retrieval (Holben et al., 1998, 2001) and serves as the ground-truth for validation of satellite data. As it is based on the assumption of a cloud-free path between instrument and sun, the identification and removal of cloud contaminated data is one of the most important prerequisites for high qualitiy AOD data.

The most widely used algorithm by Smirnov et al. (2000) sets a threshold on the temporal variation of AOD, assuming a higher variation in the presence of clouds. While this method reliably flags thick clouds, there is a limit to detect optically thin clouds exhibiting small AOD changes, i.e. below the threshold. This limitation introduces a bias towards higher AOD (Chew et al., 2011; Huang et al., 2011), as well as a bias in the Angstrom parameters which indicate particle size.

To remedy this problem without additional manual quality control, Giles et al. (2018) revised the Smirnov et al. (2000) algorithm (see table 2 of Giles et al. (2018) for specifics). They include aureole scans in their cloud screening routine which utilize the increased forward scattering behaviour of thin clouds for their identification. This is suitable for instruments that measure sky radiance in addition to direct sun. However, the procedure takes time and is only viable within AERONET who employ these instruments, whereas it is not applicable for precision filter radiometers operated within other networks, such as the WMO global atmosphere watch programme (GAW).

Therefore, we developed a new algorithm that can identify thin clouds, and works with direct sun measurements only. The main idea is that aerosol optical depth and microphysical properties (represented by the Angstrom parameters, Gobbi et al. (2007)) stay roughly constant within a day, while clouds introduce outliers in these parameters.

Instead of scanning the timeseries of these variables, we examine their density in a four-dimensional space with a k-nearest-

https://doi.org/10.5194/amt-2020-368
Preprint. Discussion started: 29 September 2020


Atmospheric Measurement Techniques Discussions

neighbours algorithm. This principle is well established in the fields of machine learning and data mining as an efficient way to identify outliers in data (Ramaswamy et al., 2000). In the context of AOD measurements, clear sky will lead to regions of high density/little distance between points, whereas clouds will result in less dense regions/outliers.

## 2 Data and Methods

### 2.1 Instrument and Raw Data

We use a precision filter radiometer (PFR) developed by the PMOD WRC Davos for the GAW network (Wehrli, 2005) with four channels (368nm, 412nm, 501nm, 864nm) and a field of view of 1.2°. The instrument is set up on top of a ten-storey university building in Innsbruck, Austria (47° 15' N, 11° 24' E). Our operational guidelines are based on the ones of GAW and the instrument is calibrated by PMOD, but our site runs independently of the network. Additional to the minutely PFR reading, we measure the air temperature and pressure at the site and monitor the overall cloud conditions with an all-sky camera taking pictures every 10 minutes.

### 2.2 Processing and filtering

First steps in quality control include the removal of data points where any of the four voltages is negative. Furthermore, flags are introduced if the sun tracker records a value higher than 15", and an ambient temperature above 310 K.
After the initial filtering, aerosol optical depth (AOD) is calculated from the voltage measurements. Starting from the Lambert-Beer law, the aerosol optical depth is derived as:

$$\tau_a(\lambda) = m_a^{-1}\Big[\ln\Big(\frac{V_0(\lambda)}{V(\lambda)R^2}\Big) - \sum_o m_o\tau_o(\lambda)\Big] \tag{1}$$

where $V(\lambda)$ are the measurements, $V_0(\lambda)$ the calibration factors, $R$ the Sun-Earth distance, and $m$ the airmass in the path between instrument and sun.
Several atmospheric constituents contribute to the optical depth, one of which are aerosols (indicated by subscript $a$). Other factors (subscript $o$) which are taken into account in our calculation are Rayleigh scattering (Kasten and Young, 1989; Bodhaine et al., 1999), Ozone (Komhyr et al., 1989), and $NO_2$ (Valks et al., 2011). We use climatological values for $O_3$ and $NO_2$, and temperature and pressure measured on site.
Resulting unphysical values (negative or infinite) of the aerosol optical depth are discarded.
At each timestep, we perform a linear and a quadratic fit (indicated with subscripts $l$ and $q$ respectively) to $\tau_a(\lambda)$ to derive the Angstrom parameters (Ångström, 1929, 1964; King and Byrne, 1976).

$$\ln\big(\tau_a(\lambda)\big) = \ln(\beta_l) - \alpha_l\ln(\lambda) \tag{2}$$

$$\ln\big(\tau_a(\lambda)\big) = \ln(\beta_q) - \alpha_q\ln(\lambda) + \gamma_q\ln(\lambda)^2 \tag{3}$$

https://doi.org/10.5194/amt-2020-368
Preprint. Discussion started: 29 September 2020


Atmospheric Measurement Techniques Discussions

The spectral slope $\alpha_l$ of the linear fit and the spectral curvature $\gamma_q$ of the quadratic fit are used in further analysis and referred to without the subscript hereafter.

### 2.3 Cloud flagging

The next step in quality control of the data is the flagging of potentially cloud-contaminated datapoints. Figure 1 shows the basic principle of the presently employed scheme and the proposed new method.

Currently, our operational routine is based on the criteria laid out in Smirnov et al. (2000), with some minor adaptions according to Wuttke et al. (2012). The main criterion for filtering datapoints is the difference between the maximum and minimum AOD value within a multiplet of consecutive datapoints (Smirnov et al. (2000) uses a triplet, whereas we look at a quintuplet) which cannot exceed a set value. This threshold is balanced to filter clouds while retaining real AOD variations. As this criterion is the most relevant for flagging, we will refer to it as "Multiplet routine" hereafter.

Instead of step-wise scanning timeseries, our new routine performs one calculation for all currently available datapoints. We use a $k$-nearest neighbours algorithm to establish the 20 closest points $\{P_1, P_2, ..., P_{20}\}$ for each of our measurements $P_0$ in a four dimensional space. Then the mean euclidian distance between $P_0$ and its neighbours is calculated (referred to as $d_{20}$) and $P_0$ is identified as cloudy if this distance exceeds a threshold. This method is usually used to identify clusters of data points, hence we will call it "Clustering routine".

The dimensions used are the aerosol optical depth at 501nm, its first derivative with respect to time, and the two Angstrom parameters $\alpha$ and $\gamma$. The first two cover temporal variations of one wavelength, the second two changes in the spectrum. To ensure that these parameters are comparable in order of magnitude, the Angstrom parameters derived from equations 2 and 3 are divided by a factor of 10. Furthermore, the finite-difference time derivative of the AOD is used in units of 1 per 5 minutes, analoguous to checking the AOD variation within a quintuplet of measurements.

Points affected by a track error will not be considered in the set of possible nearest neighbours. If less than 20 measurements are valid, the number of nearest neighbours $k$ will be reduced accordingly down to a minimum value of 5 points in real-time analysis. To account for the lower number of nearest neighbours, the calculated distance is then multiplied by $\frac{20}{k}$ to make it comparable to the $d_{20}$ measure. Similarly, if the number of datapoints identified as clear on one particular day is lower than 30, the Clustering routine is re-run with 10 nearest neighbours during post-processing to ensure high data retention.

To establish the threshold for possible cloud contamination, we calculate the distribution of $d_{20}$ on clear days. We estimate a limit, which is further fine tuned using days on which the Multiplet routine fails to identify thin clouds. An example ($12^{\text{th}}$ March 2020) is given in figure 2. We show the four dimensions of our space, as well as the resulting $d_{20}$ of our datapoints. From these days, we set the $d_{20}$ threshold to 0.012.

## 3 Results and Discussion

To assess the performance of the Clustering routine, we will compare it to the Multiplet routine, using the last 10 years of measurements (2010-2019), with 3330 days of measurements in total. Of these days, 1906 are found to have clear datapoints

https://doi.org/10.5194/amt-2020-368
Preprint. Discussion started: 29 September 2020


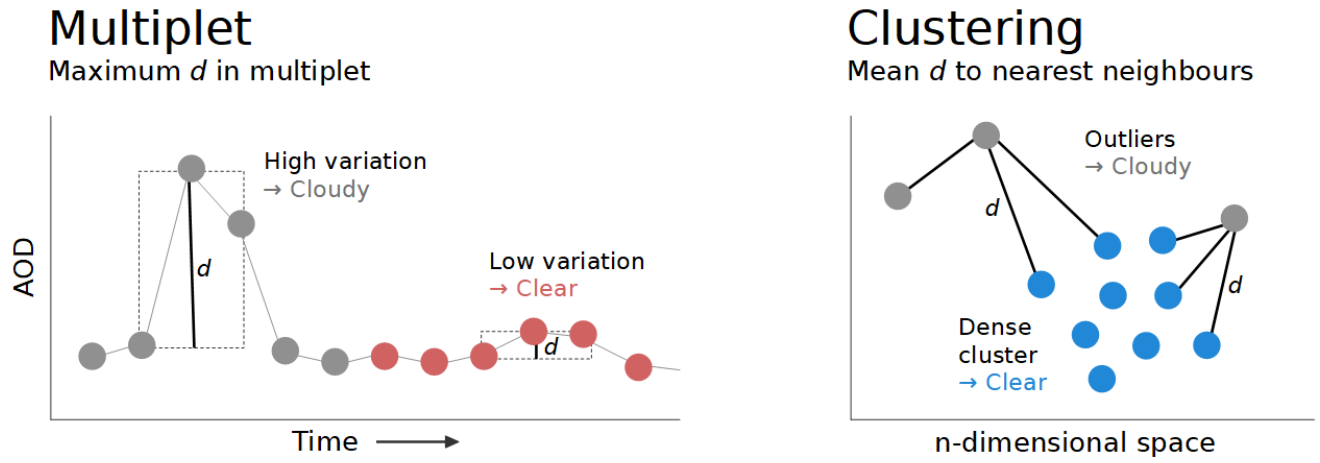


**Figure 1.** Schematics of the cloud screening methods. Left: The Multiplet method evaluates the difference between maximum and minimum AOD value of a set number of consecutive datapoints. Right: The Clustering method calculates the mean distance to $k$ nearest neighbours in an n-dimensional space. Points for which a certain threshold of the respective measure $d$ (indicated with the solid black lines) is passed will be identified as cloudy. These points are coloured in grey, wheras the clear points are coloured red/blue for Multiplet/Clustering.

by at least one routine.

To exemplify the similarities and differences of the two routines, figure 3 shows days with different cloud and aerosol conditions: clear, intermittent thick clouds, intermittent thin clouds, a combination of passing thick and thin clouds, Saharan dust, and volcanic ash. Depicted are the timeseries of AOD at 501nm as well as a scatterplot of the Angstrom parameters $\alpha$ and $\gamma$ for five days. Additional examples are shown in figure A1.

On a clear day, the routines agree unsurprisingly very well. Clustering retains more points at the beginning and end of the day, which get picked up by limiting the airmass in the Multiplet routine. On the other hand, some slight outliers in $\alpha$ and $\gamma$ get flagged by Clustering. The difference in daily mean is smaller than the measurement error.

When thick clouds are passing, with just short intervals of clear sky in between, Multiplet hardly identifies these as such. As Clustering takes all available data into account, it can assign points as clear even if the immediately preceeding and consecutive point are deemed cloudy. Despite flagging less points, Clustering lowers the daily mean $\tau_{501}$ by 0.008 in this case, which is of similar magnitude as our measurement error.

On a day with lots of thin clouds (mainly contrails), the differences between the two routines are pronounced: a few relatively high AOD points in the morning (around 8am) pass Clustering, as do points during midday (between 10am and 12am). These points, which are spectrally very similar, are indeed cloud free, as confirmed by pictures of the sky camera. Multiplet however, filters less points as cloudy, which show cloud contamination as a decrease in fine mode fraction in the $\alpha$-$\gamma$ plane. For this day, the Clustering-Multiplet difference of daily mean $\tau_{501}$ is -0.027, which is the order of possible bias of Multiplet reported by Chew et al. (2011).

Another example of Clustering being more rigorous in cloud flagging can be seen on the day labelled with "Various Clouds".

https://doi.org/10.5194/amt-2020-368
Preprint. Discussion started: 29 September 2020


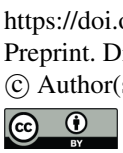

Atmospheric Measurement Techniques Discussions

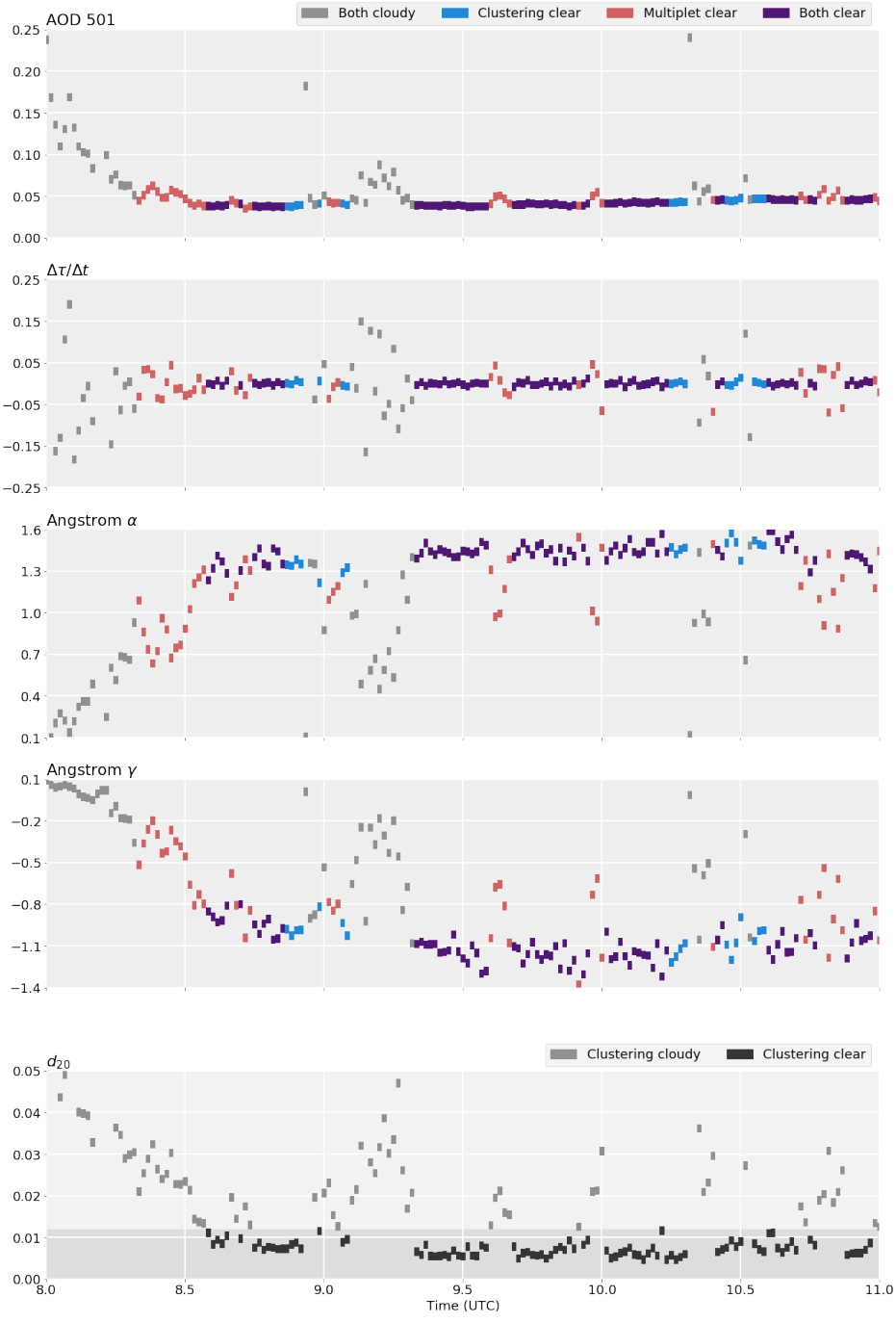


**Figure 2.** Three hours of an example day (12th March 2020) to illustrate the Clustering method: Timeseries of the four dimensions used, as well as the timeseries of the distance measure $d_{20}$. Colour of the rectangles codes for the flagging of the datapoint (see legend). For the distance measure $d_{20}$, points below the threshold, i.e. categorized as clear by Clustering, are coloured dark grey, cloudy points in light grey.

https://doi.org/10.5194/amt-2020-368
Preprint. Discussion started: 29 September 2020


Atmospheric Measurement Techniques Discussions

There were several optically thick clouds passing, which get identified correctly, but neither their thin edges nor the optically thin clouds on that day get picked up by the Multiplet routine. This day gets correctly eliminated by Clustering despite Multiplet marking 89 datapoints as clear.

Occasionally, Saharan Dust can get transported to Austria. Despite unusually high AOD, both routines correctly identify most of the data as cloud free. Daily mean $\tau_{501}$ is slightly lower (-0.005) when using Clustering, but this is still of the order of the calibration error.

One very unusual event is depicted last: after the eruption of Eyjafjallajökull in Iceland in April 2010, its ash plume was dispersed over Europe. It exhibits high AOD, and similar particle radii and fine mode fraction as Sahara dust. Clustering flags more data due to the high variation in AOD with time, but still retains data in the afternoon after about 1pm. Unfortunately, we do not have pictures available to estimate whether the data in the morning was cloud free, and should therefore be retained. Clustering lowers daily mean $\tau_{501}$ significantly, leading to -0.057 absolute and -12% relative difference. However, such an event is rare enough to be manually cloud screened, if necessary.

Overall, the Clustering routine flags more data than the Multiplet routine, albeit not necessarily the same data points. A more detailed comparison can be seen in figure 4. The Multiplet routine identifies about 47.6% of datapoints as cloudy, Clustering about 50.5%, which is a realistic value considering the amount of sunshine hours Innsbruck receives on average.

As the main objective of the new algorithm was to filter thin clouds which previously passed the quality criteria, a higher number of flagged datapoints overall is expected. On the other hand, Clustering can flag isolated outliers without flagging the preceding and succeeding points of the multiplet, which lowers the number of flagged points. In 88% of all cases, the two methods agree in the (non-)assignment of a cloudflag. Nonetheless, about 10% of the data deemed cloudy by Multiplet is not flagged by Clustering, whereas 15% of the data passing the Multiplet criteria is identified as cloudy by Clustering.

The mean AOD values of all clear points based on Multiplet flagging are $\bar{\tau}_{368} = 0.19$, $\bar{\tau}_{412} = 0.16$, $\bar{\tau}_{501} = 0.13$, and $\bar{\tau}_{368} = 0.05$. The respective values based on Clustering do not differ significantly, which is partly due to the low number of datapoints on which the routines disagree.

On daily timescales, Clustering eliminates 169 days for which Multiplet would still find valid datapoints. On the other hand, there are only 10 days where the opposite is the case. Nonetheless, there are more than 1000 days without clear data in the 10-year record. The number of datapoints on the days which are disregarded by Clustering ranges between 1 and 89. Most of these days would therefore not be considered in further analysis in other measurement networks (Kazadzis et al., 2018; Giles et al., 2018) either. Furthermore, as shown in Figure 3, some of these days should be eliminated as they are indeed cloud contaminated.

Clustering leads to lower daily mean AOD on about 63% of the days (Figure 5). The mean difference is -0.0029 for $\bar{\tau}_{501}$, which is of the order of the calibration error (0.001 to 0.01, depending on wavelength and airmass). However, on particular days this difference can range from -0.08 to 0.04 in absolute numbers, or -62% to +27% relative to the values based on Multiplet screening. Similarly, Clustering leads to higher mean $\alpha$ on 67% of the days. Averaged over ten years of data this leads to an increment of $\bar{\alpha}$ by 0.02. In extreme cases, the difference can be as high as +0.54. Both distributions are indicative of Clustering flagging thin clouds which Multiplet cannot properly detect.

https://doi.org/10.5194/amt-2020-368
Preprint. Discussion started: 29 September 2020


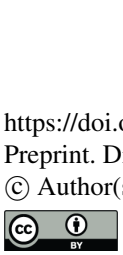

Atmospheric Measurement Techniques Discussions

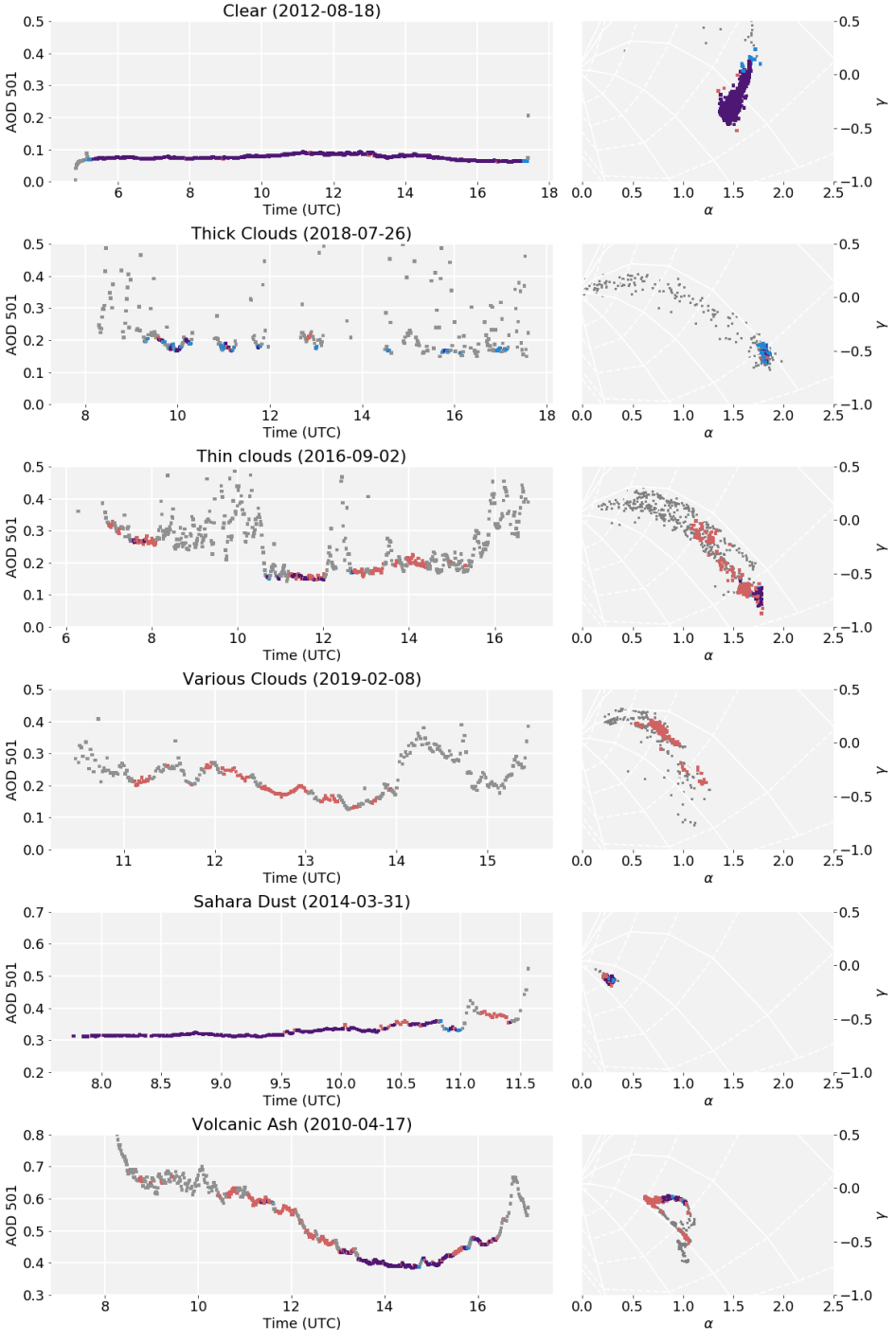


**Figure 3.** Comparison of cloud flagging routines on selected days with different cloud conditions as signified in the respective title. Colours as in Figure 2. Left: Timeseries of AOD at 501nm, Right: $\alpha$-$\gamma$-plots. The black lines show different particle radii, the white dotted lines different fine mode fractions, grid adapted from Gobbi et al. (2007). Note the different x-axis scales for the timeseries.

https://doi.org/10.5194/amt-2020-368
Preprint. Discussion started: 29 September 2020


Atmospheric Measurement Techniques Discussions

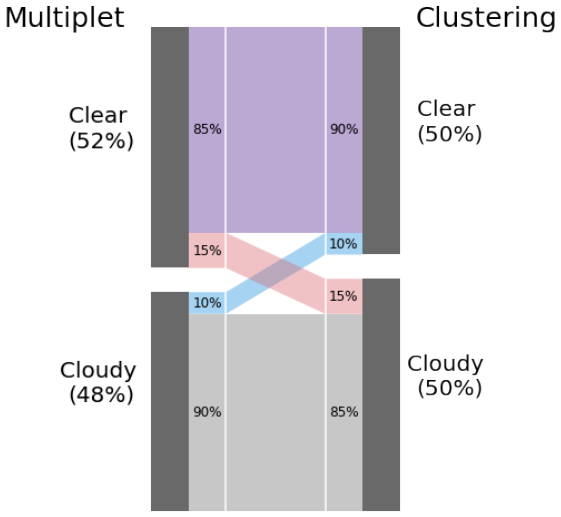


**Figure 4.** Comparison of flagging by the two routines. The height of each area is proportional to the total number of datapoints in each category. Grey: Both routines classify as cloudy, Red/Blue/Purple: Multiplet/Clustering/Both classify as clear.

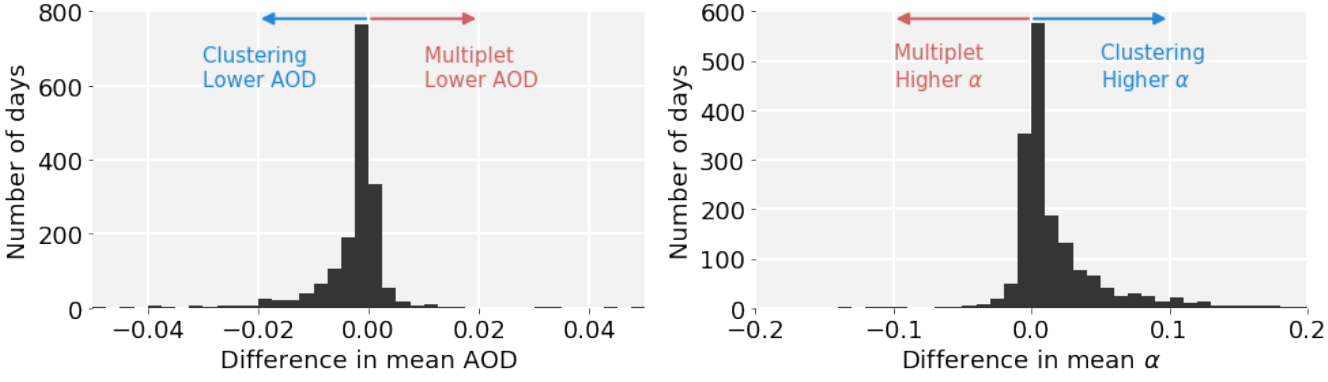


**Figure 5.** Histogram of the Clustering-Multiplet difference in daily mean of AOD at 501nm (left) and of $\alpha$ (right). Negative/positive values mean that the daily mean is lower/higher when screened by Clustering.

https://doi.org/10.5194/amt-2020-368
Preprint. Discussion started: 29 September 2020


Atmospheric Measurement Techniques Discussions

## 4 Conclusions

We presented a new approach for flagging cloud contaminated data points from sun photometer measurements by treating them as outliers/region of low density in a four-dimensional space. Our method successfully tackles the problem of the Multiplet routine by Smirnov et al. (2000) of not detecting optically thin clouds, such as cirrus and contrails.

In contrast to the new routine employed by AERONET (Giles et al., 2018), which introduces more quality parameters (ten in total) and requires an aureole scan, our routine only needs one semi-empirically derived threshold and direct sun measurements for assigning a cloud flag.

While fewer datapoints are retained overall, which is expected from being able to filter thin clouds, the Clustering routine does not just flag more, but different datapoints (figure 4). As there is an ambiguity in the transition between humidified aerosols and clouds (Koren et al., 2007), an exact discrimination between false positives and negatives for either routine is not possible. Nonetheless, the new routine leads to lower AOD and higher $\alpha$ in the long term mean, which indicates a reduction of cloud contamination bias.

Detailed comparison with the previously employed cloud screening routine showed that both methods agree in their classification for the vast majority of cases (figure 4). Still, Clustering reduces mean AOD for most of the days in our testing period (figure 5). The daily mean AOD at 501nm averaged over the last 10 years is lowered by 0.0029, which is comparable to instrument precision (Wuttke et al., 2012). However, on single days Clustering reduces daily mean by more than 0.02 (up to 0.08), which is the same magnitude as reported as bias of the Multiplet routine by Chew et al. (2011), and exceeds the error of the instrument and trace gas optical depth. Together with specific example days (figure 3), this supports the notion that clustering corrects some cloudy points of the Multiplet routine to clear, while flagging some of its erroneously clear points as cloudy. The small difference in the long term mean is partly due to the specific cloud conditions in Innsbruck, and could therefore be much larger in high latitude regions with low mean AOD and higher prevalence of thin clouds.

Due to the nature of the Clustering routine, it needs a minimum number of measurements, though dynamic adaptions can be made if these are not available. As its accuracy increases with a higher number of datapoints, it is ideal for post-processing. This does not diminish its usefulness for real-time analysis, as erroneously cloudy points can be cleared later when more data is available, but not the other way round.

While the four dimensions considered in the Clustering routine account for variations of one specific wavelength and in the spectrum, the question arises whether these can be reduced even further. Especially $\gamma$, which has the highest error of the variables (Gobbi et al., 2007), might be a candidate. Initial independence tests using mutual conditional information as measure (Runge et al., 2019) show a strong association of $\alpha$ and $\gamma$. However, outliers in $\gamma$ can appear independently of $\alpha$, which is why we kept $\gamma$ as a dimension and therefore data constraint.

So far we have tested the routine only for our specific measurement site. It performs well in different cloud conditions, as shown in figure 3, and was shown to alleviate AOD bias in the presence of thin clouds. Adaptations regarding the number of nearest neighbours, the relative weight of the different dimensions, or the $d_{20}$ threshold can be easily done to optimize cloud detection with other instruments as well.

https://doi.org/10.5194/amt-2020-368
Preprint. Discussion started: 29 September 2020


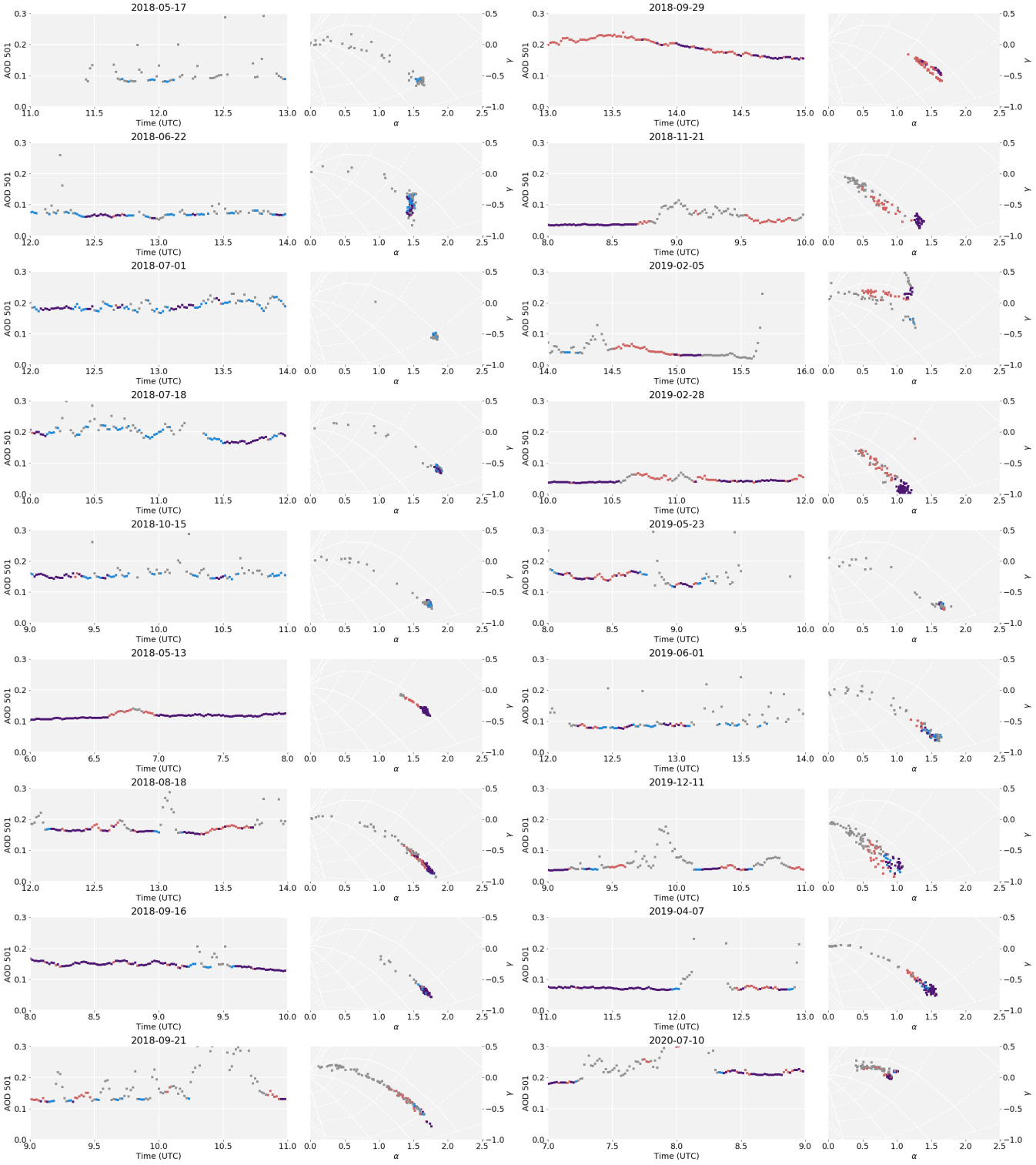


**Figure A1.** 2 hour exerpts from selected days, additionally to figure 3. The first five examples highlight cases where Clustering flags much less than Multiplet, the others show the performance in the presence of thin clouds. Both categories are ordered by date.

https://doi.org/10.5194/amt-2020-368
Preprint. Discussion started: 29 September 2020

Atmospheric Measurement Techniques Discussions

*Author contributions.* VS designed, implemented, and evaluated the Clustering algorithm. AK provided the raw data record. Both authors participated in writing, figure design, and interpretation of the results.

*Competing interests.* The authors declare that they have no conflict of interest.

https://doi.org/10.5194/amt-2020-368
Preprint. Discussion started: 29 September 2020


Atmospheric Measurement Techniques Discussions

## References

Ångström, A.: On the Atmospheric Transmission of Sun Radiation and on Dust in the Air, Geografiska Annaler, 11, 156–166, https://doi.org/10.1080/20014422.1929.11880498, 1929.

Ångström, A.: The parameters of atmospheric turbidity, Tellus, 16, 64–75, https://doi.org/10.3402/tellusa.v16i1.8885, 1964.

Bodhaine, B. A., Wood, N. B., Dutton, E. G., and Slusser, J. R.: On Rayleigh Optical Depth Calculations, Journal of Atmospheric and Oceanic Technology, 16, 1854–1861, https://doi.org/10.1175/1520-0426(1999)016<1854:ORODC>2.0.CO;2, 1999.

Chew, B. N., Campbell, J. R., Reid, J. S., Giles, D. M., Welton, E. J., Salinas, S. V., and Liew, S. C.: Tropical cirrus cloud contamination in sun photometer data, Atmospheric Environment, 45, 6724 – 6731, https://doi.org/https://doi.org/10.1016/j.atmosenv.2011.08.017, 2011.

Giles, D., Sinyuk, A., Sorokin, M., Schafer, J., Smirnov, A., Slutsker, I., Eck, T., Holben, B., Lewis, J., Campbell, J., Welton, E., Korkin, S., and Lyapustin, A.: Advancements in the Aerosol Robotic Network (AERONET) Version 3 Database – Automated Near Real-Time Quality Control Algorithm with Improved Cloud Screening for Sun Photometer Aerosol Optical Depth (AOD) Measurements, Atmospheric Measurement Techniques Discussions, pp. 1–78, https://doi.org/10.5194/amt-2018-272, 2018.

Gobbi, G. P., Kaufman, Y. J., Koren, I., and Eck, T. F.: Classification of aerosol properties derived from AERONET direct sun data, Atmospheric Chemistry and Physics, 7, 453–458, https://doi.org/10.5194/acp-7-453-2007, https://www.atmos-chem-phys.net/7/453/2007/, 2007.

Holben, B., Eck, T., Slutsker, I., Tanré, D., Buis, J., Setzer, A., Vermote, E., Reagan, J., Kaufman, Y., Nakajima, T., Lavenu, F., Jankowiak, I., and Smirnov, A.: AERONET—A Federated Instrument Network and Data Archive for Aerosol Characterization, Remote Sensing of Environment, 66, 1 – 16, https://doi.org/https://doi.org/10.1016/S0034-4257(98)00031-5, 1998.

Holben, B. N., Tanré, D., Smirnov, A., Eck, T. F., Slutsker, I., Abuhassan, N., Newcomb, W. W., Schafer, J. S., Chatenet, B., Lavenu, F., Kaufman, Y. J., Castle, J. V., Setzer, A., Markham, B., Clark, D., Frouin, R., Halthore, R., Karneli, A., O'Neill, N. T., Pietras, C., Pinker, R. T., Voss, K., and Zibordi, G.: An emerging ground-based aerosol climatology: Aerosol optical depth from AERONET, Journal of Geophysical Research: Atmospheres, 106, 12 067–12 097, https://doi.org/10.1029/2001JD900014, 2001.

Huang, J., Hsu, N. C., Tsay, S.-C., Jeong, M.-J., Holben, B. N., Berkoff, T. A., and Welton, E. J.: Susceptibility of aerosol optical thickness retrievals to thin cirrus contamination during the BASE-ASIA campaign, Journal of Geophysical Research: Atmospheres, 116, https://doi.org/10.1029/2010JD014910, 2011.

Kasten, F. and Young, A. T.: Revised optical air mass tables and approximation formula, Appl. Opt., 28, 4735–4738, https://doi.org/10.1364/AO.28.004735, 1989.

Kazadzis, S., Kouremeti, N., Nyeki, S., Gröbner, J., and Wehrli, C.: The World Optical Depth Research and Calibration Center (WORCC) quality assurance and quality control of GAW-PFR AOD measurements, Geoscientific Instrumentation, Methods and Data Systems, 7, 39–53, https://doi.org/10.5194/gi-7-39-2018, 2018.

King, M. D. and Byrne, D. M.: A Method for Inferring Total Ozone Content from the Spectral Variation of Total Optical Depth Obtained with a Solar Radiometer, Journal of the Atmospheric Sciences, 33, 2242–2251, https://doi.org/10.1175/1520-0469(1976)033<2242:AMFITO>2.0.CO;2, 1976.

Komhyr, W. D., Grass, R. D., and Leonard, R. K.: Dobson spectrophotometer 83: A standard for total ozone measurements, 1962–1987, Journal of Geophysical Research: Atmospheres, 94, 9847–9861, https://doi.org/10.1029/JD094iD07p09847, 1989.

Koren, I., Remer, L. A., Kaufman, Y. J., Rudich, Y., and Martins, J. V.: On the twilight zone between clouds and aerosols, Geophysical Research Letters, 34, https://doi.org/10.1029/2007GL029253, 2007.

https://doi.org/10.5194/amt-2020-368
Preprint. Discussion started: 29 September 2020


Atmospheric Measurement Techniques Discussions

Ramaswamy, S., Rastogi, R., and Shim, K.: Efficient Algorithms for Mining Outliers from Large Data Sets, SIGMOD Rec., 29, 427–438, https://doi.org/10.1145/335191.335437, https://doi.org/10.1145/335191.335437, 2000.

Runge, J., Nowack, P., Kretschmer, M., Flaxman, S., and Sejdinovic, D.: Detecting and quantifying causal associations in large nonlinear time series datasets, Science Advances, 5, https://doi.org/10.1126/sciadv.aau4996, 2019.

Smirnov, A., Holben, B., Eck, T., Dubovik, O., and Slutsker, I.: Cloud-Screening and Quality Control Algorithms for the AERONET Database, Remote Sensing of Environment, 73, 337–349, https://doi.org/https://doi.org/10.1016/S0034-4257(00)00109-7, 2000.

Valks, P., Pinardi, G., Richter, A., Lambert, J.-C., Hao, N., Loyola, D., Van Roozendael, M., and Emmadi, S.: Operational total and tropospheric $NO_2$ column retrieval for GOME-2, Atmospheric Measurement Techniques, 4, 1491–1514, https://doi.org/10.5194/amt-4-1491-2011, https://www.atmos-meas-tech.net/4/1491/2011/, 2011.

Wehrli, C.: GAWPFR: A Network of Aerosol Optical Depth Observatioins with Precision Filter Radiometers, in: WMO/GAW experts workshop on a clobal surface-based network for long term observations of column aerosol optical properties, edited by Baltensperger, U., Barrie, L., and Wehrli, C., no. 162 in GAW Report, pp. 36–39, 2005.

Wuttke, S., Kreuter, A., and Blumthaler, M.: Aerosol climatology in an Alpine valley, Journal of Geophysical Research: Atmospheres, 117, https://doi.org/10.1029/2012JD017854, 2012.